

C. Lacasse · S. Karlsdóttir · G. Larsen · H. Soosalu ·
W. I. Rose · G. G. J. Ernst

Weather radar observations of the Hekla 2000 eruption cloud, Iceland

Received: 10 May 2003 / Accepted: 23 October 2003 / Published online: 12 December 2003
© Springer-Verlag 2003

Abstract The Hekla eruption cloud on 26–27 February 2000 was the first volcanic cloud to be continuously and completely monitored advecting above Iceland, using the C-band weather radar near the Keflavík international airport. Real-time radar observations of the onset, advection, and waning of the eruption cloud were studied using time series of PPI (plan-position indicator) radar images, including VMI normal, Echotop, and Capi level 2

displays. The reflectivity of the entire volcanic cloud ranges from 0 to >60 dBz. The eruption column above the vent is essentially characterised by VMI normal and Capi level 2 values, >30 dBz, due to the dominant influence of lapilli and ash (tephra) on the overall reflected signal. The cloud generated by the column was advected downwind to the north-northeast. It is characterised by values between 0 and 30 dBz, and the persistence of these reflections likely result from continuing water condensation and freezing on ash particles. Echotop radar images of the eruption onset document a rapid ascent of the plume head with a mean velocity of ~30 to 50 m s⁻¹, before it reached an altitude of ~11–12 km. The evolution of the reflected cloud was studied from the area change in pixels of its highly reflected portions, >30 dBz, and tied to recorded volcanic tremor amplitudes. The synchronous initial variation of both radar and seismic signals documents the abrupt increase in tephra emission and magma discharge rate from 18:20 to 19:00 UTC on 26 February. From 19:00 the >45 dBz and 30–45 dBz portions of the reflected cloud decrease and disappear at about 7 and 10.5 h, respectively, after the eruption began, indicating the end of the decaying explosive phase. The advection and extent of the reflected eruption cloud were compared with eyewitness accounts of tephra fall onset and the measured mass of tephra deposited on the ground during the first 12 h. Differences in the deposit map and volcanic cloud radar map are due to the fact that the greater part of the deposit originates by fallout off the column margins and from the base of the cloud followed by advection of falling particle in lower level winds.

Editorial responsibility: P. Mouginis-Mark

C. Lacasse (✉)
Volcano Dynamics Group, Department of Earth Sciences,
The Open University,
Walton Hall, Milton Keynes, MK7 6AA, UK
e-mail: c.m.lacasse@open.ac.uk
Tel.: +44-1908-652118
Fax: +44-1908-655151

S. Karlsdóttir
Icelandic Meteorological Office,
Bustadavegur 9, 150 Reykjavík, Iceland

G. Larsen
Science Institute,
University of Iceland,
Dunhaga 3, 107 Reykjavík, Iceland

H. Soosalu
Nordic Volcanological Institute,
Grensásvegur 50, 108 Reykjavík, Iceland

W. I. Rose · G. G. J. Ernst
Department of Geological Engineering and Sciences,
Michigan Technological University,
1400 Townsend Drive, Houghton, Michigan 49931, USA

G. G. J. Ernst
Centre for Environmental and Geophysical Flows,
Department of Earth Sciences,
University of Bristol,
Wills Memorial Building, Queen's Road, Bristol, BS8 1RJ, UK

Present address:

G. G. J. Ernst, Department of Geology and Soil Science,
Research Centre for Eruption Dynamics,
University of Ghent,
Krijgslaan 281, S8, 9000, Ghent, Belgium

Keywords Hekla 2000 eruption · Iceland · Volcanic cloud · Radar observations · Tephra fall · Volcanic tremor · Aircraft safety

Introduction

In a recent paper by Grindle and Burcham (2002), the encounter of the Hekla 2000 eruption cloud with a NASA McDonnell-Douglas DC8 research aircraft was reported, with the degree of damage being severe enough that all four engines had to be refurbished. Although there was controversy about the interpretations at first [see discussion in Pieri et al. (2002)], atmospheric instrument particle sampling data and IR remote sensing reported by Rose et al. (2003) and SEM analyses of aircraft ventilation filters (Pieri et al. 2002) are all consistent with there being volcanic ash in the encountered eruption cloud. Rose et al. (2003) estimated the mass of fine ash at about 100 kT. Ice nucleated on the surface of ash particles and it is likely that most of the particle mass in the Hekla eruption cloud is ice [see Rose et al. (2003) for discussion on this topic]. This incident brought to attention the fact that complete avoidance of volcanic clouds is indeed the only procedure that guarantees flight safety (Cantor 1998). Volcanic eruptions in Iceland pose a major hazard to the traffic of jet aircraft in the subpolar North Atlantic-Arctic region, which is one of the most heavily trafficked air corridors in the world. Prior to this recent incident and in spite of eruptions occurring in Iceland once every 4 or 5 years on average, no encounter between commercial aircraft and eruption clouds had been officially reported in the region. On average, about 250 jet planes per day fly across the Icelandic Oceanic Control Area (IOCA) in the North Atlantic and in favourable meteorological conditions this number can double (Sveinbjörnsson 2001). Thus, there is an urgent need to improve the capability of measuring and tracking volcanic clouds from Iceland using radar and satellite remote sensing (see Rose et al. 2003). The Hekla eruption cloud in January 1991 was the first to be detected over Iceland by the Keflavík C-band weather radar. The radar located near the international airport began operation a few days prior to the eruption (Larsen et al. 1992). However, as the Hekla 2000 radar data set is more complete than that of 1991, we concentrate here instead on the 2000 eruption. The radar detected the Hekla 2000 eruption cloud and also comprehensively monitored its advection and waning phases above Iceland. The data set is also the first extensive C-band radar data set of a volcanic cloud to be documented with such high time resolution, and provides new and unique constraints for the future evaluation of models on volcanic plume dynamics and microphysics. This study makes a strong case for a more extensive use of weather radars in future monitoring and studies of volcanic clouds and their dynamics. In this paper, we present the first results of real-time radar observations of the 2000 Hekla eruption cloud using the C-band Keflavík weather radar operated by the Icelandic Meteorological Office (IMO). Radar images of the eruption cloud, acquired every 5 min during the first 12 h after the eruption's onset at 18:17, were studied and compared with ground observations of the tephra fall (Árnason 2002; Haraldsson 2001; Haraldsson et al. 2002; G. Larsen, unpublished data, 2003) and

recorded volcanic tremor amplitudes (Soosalu et al. 2002; H. Soosalu, unpublished data, 2003). For consistency in our study we use the term “volcanic (eruption) cloud” to generically refer to both the eruption column and the derived wind-advected cloud, whereas the term “volcanic (eruption) plume” was used to describe its buoyancy-dominated region (Sparks et al. 1997).

Specifications and detection limits of the weather radar at Keflavík, SW Iceland

Specifications

The weather radar is an Ericsson C-band radar (EWIS II). It is located about 3 km north of the Keflavík international airport in southwest Iceland and has been in operation since January 1991 (Figs. 1 and 2a). It monitors cloud cover and precipitation within a maximum radius of 480 km from its location. Description and specifications of the radar system are given in Table 1 and its range is illustrated in Fig. 2b. Weather radars usually display on-

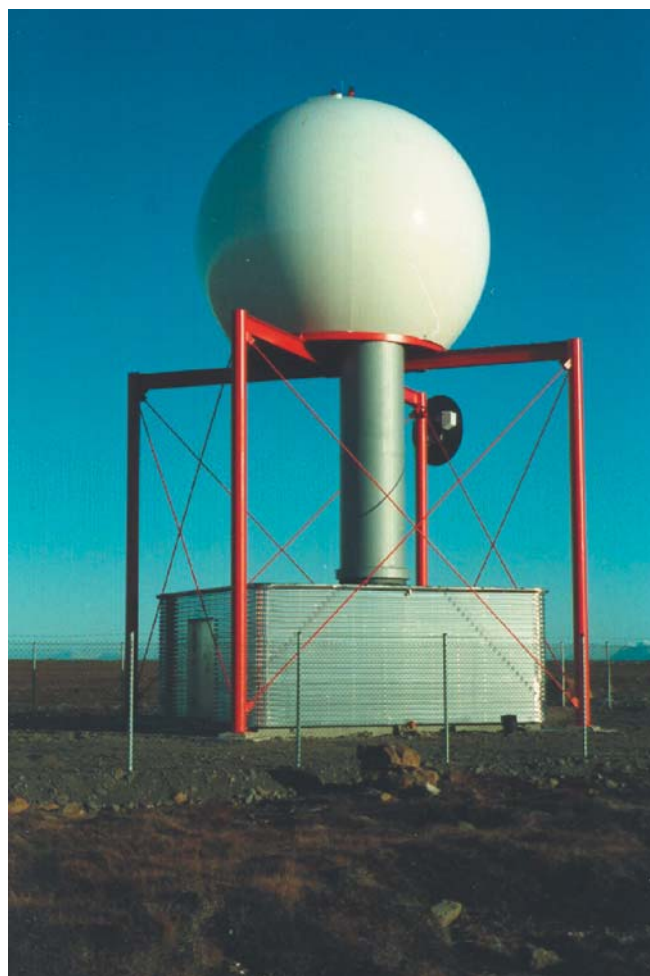


Fig. 1 View of the weather radar near Keflavík international airport, southwest Iceland. (Courtesy of F.H. Sigurdsson)

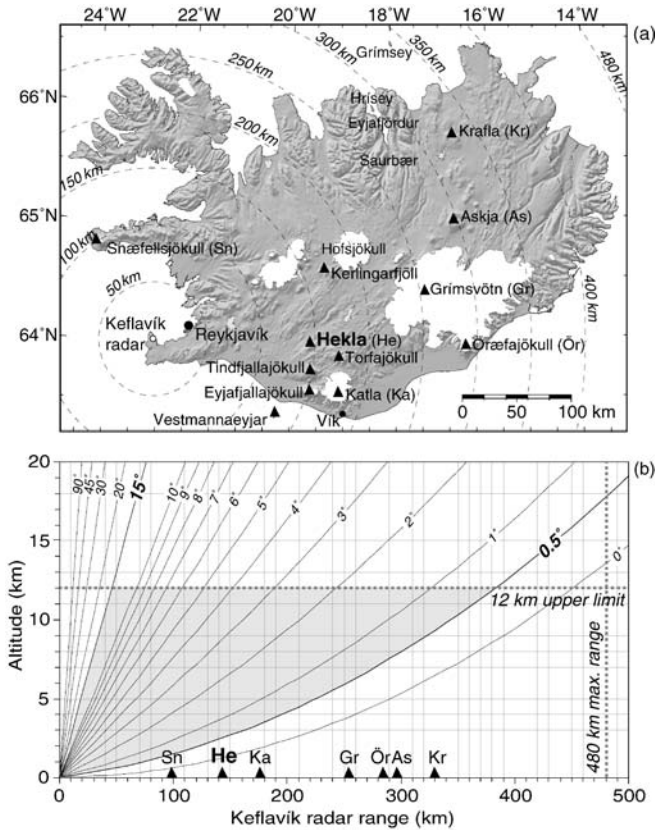


Fig. 2 **a** Location map of the Keflavík radar and major volcanoes in Iceland. **b** Range-height (a.s.l.) diagram as a function of distance from the Keflavík radar to different Icelandic volcanoes. *Shaded field* shows the detection limit with the present radar configuration

Table 1 Specifications of the weather radar system in Keflavík, SW Iceland

Type	C-band Ericsson radar system EWIS
Location	64°01'35"N, 22°38'09"W
Operational since	January 1991
Height of antenna	47 m above sea level
Peak transmitted power	245.2 kW
Beam width	0.9°
Elevation angle	0.5°
Pulse duration	2.15 μ m
Wavelength	5 cm
Pulse repetition rate	250 \pm 2 Hz
Maximum range	480 km
Actual gain of antenna	44.9 dB

screen contours of equal reflectivity on both plan-position indicator (PPI) images and range-height indicator (RHI) images (e.g. see Rose and Kostinski 1994; Rose et al. 1995a). PPI and RHI images represent, respectively, a horizontal and a vertical cross section of reflecting clouds. The radar system at Keflavík is remotely operated by the IMO in Reykjavík. Currently, scanned images are routinely acquired every 20 min for normal weather monitoring and every 5 min during volcanic eruptions. At present, only scanned PPI images can be converted from

the archived data to TIF format. Among the whole range of PPI displays generated, three are currently retrieved using the present software configuration. They include vertical maximum intensity (VMI) images and constant altitude PPI (Cappi) level 2 images of the maximum reflectivity measured at all heights and at 2 km a.s.l., respectively, and Echotop images of the maximum cloud height up to 12 km a.s.l. For the first two types of data displays, the reflectivity of clouds is measured by comparing them to a standard equivalent reflectivity z expressed in decibels (dB) relative to a rain target with a reflectivity factor Z_0 of $1 \text{ mm}^6 \text{ m}^{-3}$ (see Eq. 1), for a range of natural precipitation clouds with z values of about 1 to more than 50 dB (e.g. Rinehart 1991; Houze 1993):

$$z = 10 \log_{10}(Z/Z_0), \quad \text{with } Z_0 = 1 \text{ mm}^6 \text{ m}^{-3} \quad (1)$$

For hydrological use the reflectivity factor Z ($\text{mm}^6 \text{ m}^{-3}$) is converted to rain rate R (mm h^{-1}) depending on drop size distribution and precipitation phase (see Eq. 2):

$$Z = aR^b,$$

with a, b , constants depending on the precipitation phase considered. (2)

The third type of displays are Echotop images. They show the highest vertical level from which detectable radar echoes are measured and in this case this is presently up to 12 km height a.s.l. for the Keflavík radar. Concentric circles often appear on Echotop images as a result of errors in the pixel positions due to the use of the nearest neighbour technique when converting the input data from polar coordinated to fixed position in Cartesian coordinates in the output image (Karlsson 1997).

Detection limits

To obtain a complete scanned image, the radar beam circles with an initial elevation angle of 0.5° . Its revolution is gradually raised twelve times up to a 15° angle for a whole scanning time of 2 min and with each beam revolution lasting about 10 s. Figure 3a and b respectively show the volume of an eruption column above Hekla volcano that can currently be detected between the first and the last (12th) beam revolution of a single scan. The lowest detectal height by a weather radar is a function of the elevation angle of the radar beam, the distance (i.e. range) from the radar to the target, and the earth's curvature as expressed by Eq. (3) (Rinehart 1991):

$$H = \sqrt{r^2 + R^2 + 2rR' \sin(\phi)} - R' + H_0 \quad (3)$$

where H is radar height a.s.l. (km); H_0 is height a.s.l. (km) of the radar antenna; r is range (km) from the radar; ϕ is elevation angle (degrees) of the radar beam; and $R' = 4/3 R$, with the earth's radius $R = 6,374$ km.

Using the Keflavík radar characteristics (Table 1), this relation can be used to infer the lower and upper radar detection limits above Hekla (Fig. 2b). Due to software limitation so far used for this radar, the upper detection

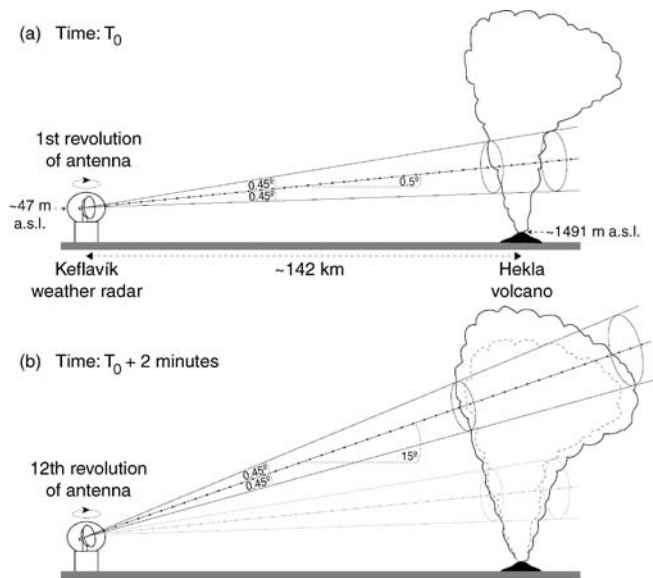


Fig. 3 Volume of the Hekla eruption column detected by the Keflavik radar of 0.9° beam width, **a** from the beginning to **b** the end of a 2-min scan

limit is imposed at 12 km height a.s.l. regardless of the detection range (Fig. 2b). Nevertheless, Fig. 2b shows that, based on the distance of ~ 142 km between the Keflavik radar ($64^\circ 01'N$, $22^\circ 38'W$) and Hekla ($63^\circ 59'N$, $19^\circ 42'W$), eruption clouds can in principle be detected to much higher elevations. Similarly, the lower detection limit can be estimated to ~ 2 km a.s.l., i.e. the eruption cloud cannot be detected between the Hekla summit at 1,491 and 2,000 m altitude with the present radar configuration. Therefore, the radar can only currently detect Hekla columns emerging across the altitude interval from 2 to 12 km (Fig. 2b). The lower and upper bounds of the Keflavik radar capability of detecting an eruption column and tracking an ash cloud generated from it strongly depend on the distance to the volcano (Fig. 2). Several active volcanoes of the South-Eastern Volcanic Zone (SEVZ) in Iceland, e.g. Eyjafjallajökull or Katla, are located within a similar range from the radar as Hekla. However, other volcanoes, e.g. Grímsvötn, Óraefajökull, and Askja, are located farther east, reducing the capability of detecting the eruption onset and the early rise of the column, or more crucially of adequately tracking the volcanic clouds in the event that they dispersed toward the northeast, east, or southeast.

Real-time radar observations of the Hekla 2000 eruption cloud

Course of events and characteristics of the eruption

Detailed accounts of the Hekla 2000 eruption can be found on the websites of the Smithsonian Global Volcanism Network (<http://www.volcano.si.edu>, exam-

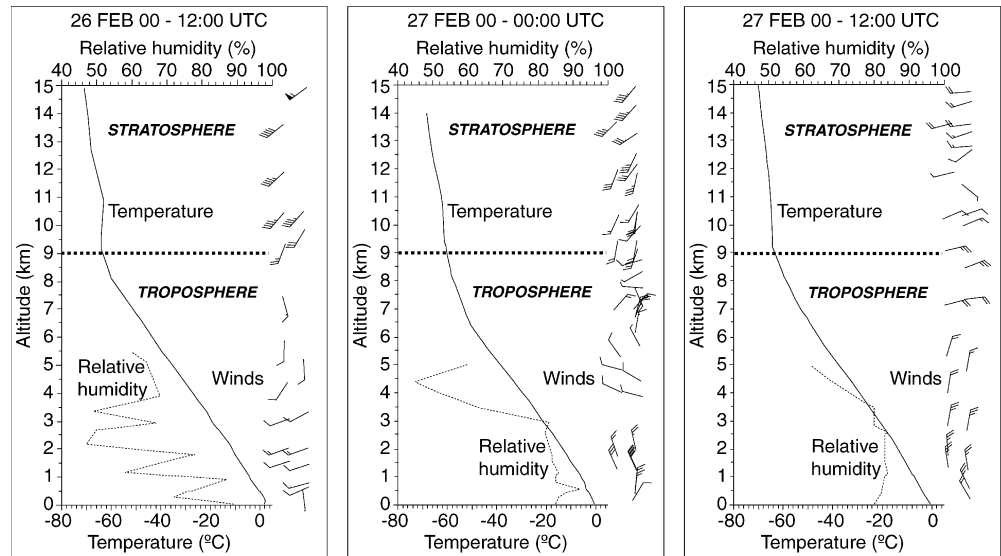


Fig. 4 View of the rising Hekla eruption column, taken near Vik (see Fig. 2a for location) at $\sim 18:35$ on 26 February 2000, at a distance of ~ 67 km from south-southeast. (Courtesy of J. Erlendsson)

ined 27 February 2003) and the Nordic Volcanological Institute (<http://www.norvol.hi.is>, examined 27 February 2003). The tephra fall and deposit, the pyroclastic flows deposits, and the evolution of the lava flows are also briefly described in Haraldsson et al. (2002), Höskuldsson and Ólafsdóttir (2002), and Ólafsdóttir et al. (2002). The 2000 eruption is considered to be the shortest and smallest of all Hekla eruptions on record according to its duration, 11 days, and the total volume of unconsolidated tephra, 0.01 km^3 , and lava, 0.17 km^3 . The bulk of the lavas were erupted in the first 48 h of activity. It is the fifth Hekla eruption in the 20th century and it also followed its shortest repose period, 9 years (since March 1991). The eruption's onset was closely preceded by a marked decrease in strain build-up rate and evidence of pressure release in the magma chamber and conduit formation system (dike), which was recorded between 18:17 and 18:19 on 26 February by a borehole strain meter some 15 km from Hekla's summit (Águstsson et al. 2000). Recent analysis by K. Águstsson (personal communication, 2003) indicates that the starting time of the eruption was close to 18:17. A 4.5-km-long fissure opened on the crest and on the southeast flank of the Hekla ridge. An eruption column that reached a maximum height of about 12 km a.s.l. (Fig. 4) was emitted from the central part of the fissure. Based on aircraft pilot reports and satellite imagery, the bulk of the volcanic cloud was initially carried at ~ 9 – 12 km height a.s.l. by southerly winds between 18.20 and $\sim 20:00$, displaying a bilobate downwind front indicating that at least a portion of the volcanic cloud flow was bifurcating (see Ernst et al. 1994; Rose et al. 2003, e.g. at 19:45 and 21:00). The erupted magma composition is basaltic andesite with minor dacite.

Due to poor weather conditions, the opening stages of the eruption and the explosive phase could not be continuously documented from the ground and air. Eyewitness accounts, photographs, and video pictures have been investigated (G. Larsen, unpublished data, 2003) and allow some conclusions on the beginning and duration of the explosive phase. The eruption began on a

Fig. 5 Rawinsonde measurements of atmospheric temperature, relative humidity, wind direction, and speed, recorded at the Keflavík meteorological station on 26 and 27 February 2000. Relative humidity only calculated up to 5 km height due to sensor defect in measuring the dew point temperature above that height, caused by very cold temperature (less than -40°C)



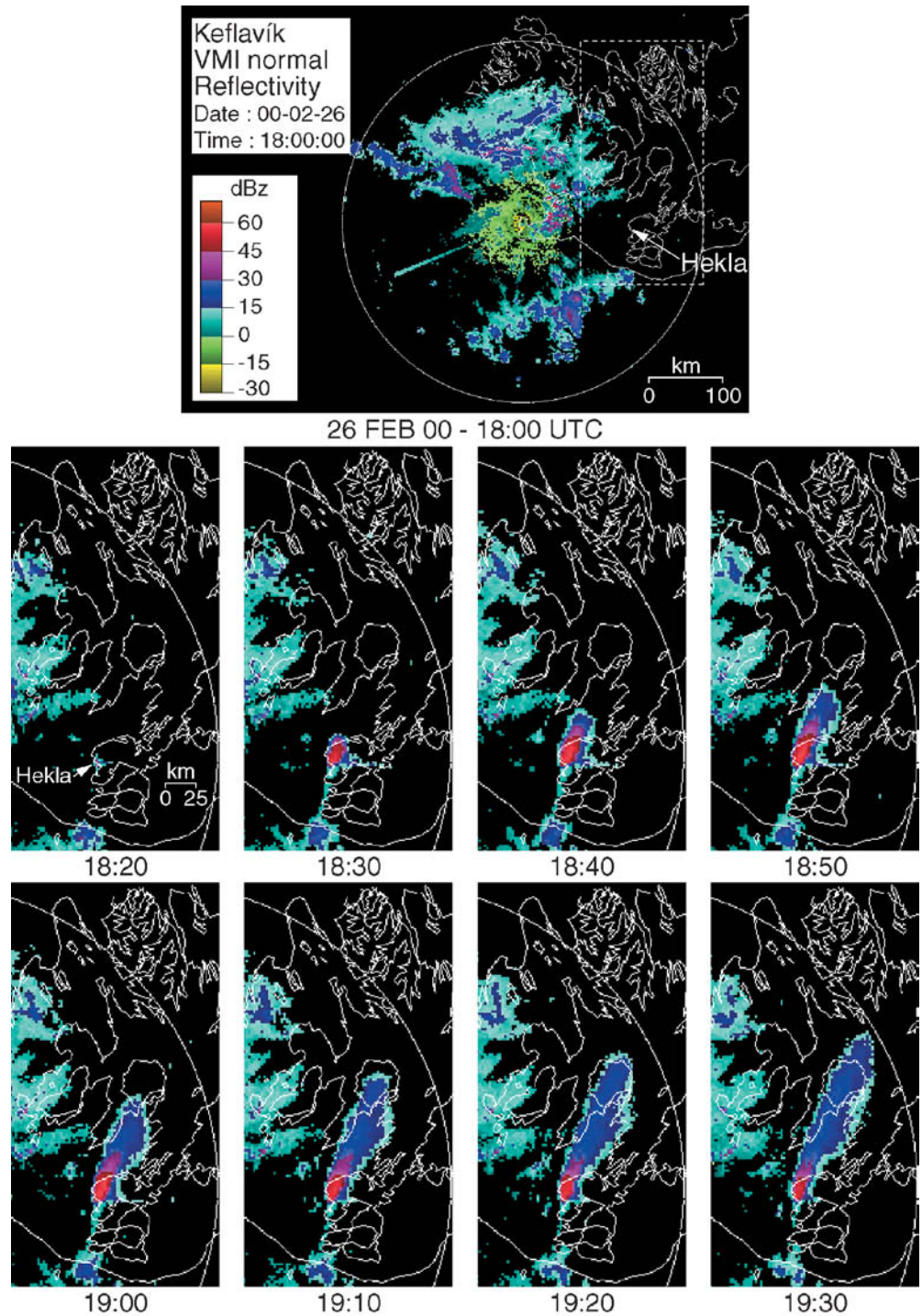
fissure segment east of the Hekla summit. At least on one occasion, the eruption column margins partially collapsed, as also occurred early in the 1980 Hekla eruption [see photographs by H.J. Beug in Grönvold et al. (1983)], locally generating small pyroclastic flow deposits, as described by Höskuldsson and Ólafsdóttir (2002). The explosive phase at the fissure's central part was subplinian at first, reaching a maximum intensity within 30 min after the eruption began (Árnason 2002; G. Larsen, unpublished data, 2003). The subplinian activity dominated during the first 90 min and was the main source of juvenile tephra that was ejected and transported by the prevailing winds towards north-northeast across central and northern Iceland and off the north coast. Elsewhere on the fissure, Hawaiian-style lava fountains dominated and this activity was still strong when the eruption was last inspected from the air at ~ 20.45 . Most of the tephra generated by the lava fountains was deposited in the vicinity of the vents. Both the explosive activity at the central part of the fissure and the Hawaiian lava fountains and Strombolian activity can be essentially accounted for by the volcanic tremors recorded during the first 12 h of the eruption (Soosalu et al. 2002; H. Soosalu, unpublished data, 2003). The initial subplinian phase is of great interest for volcanological and air safety reasons as it generated an eruption column with its top at $\sim 11\text{--}12$ km height a.s.l. reaching the lower stratosphere, with the tropopause above Iceland at $8\text{--}9$ km height a.s.l. in February [see Fig. 5 and Lacasse (2001)]. In the waning stages of subplinian activity, the decrease in eruption intensity may have enabled groundwater to enter the fissure conduit, leading to a shift from a dry subplinian eruption driven by extreme magmatic degassing and magmatic gas expansion to phreatomagmatic activity, with more frequent steam explosions due to the increasing role of groundwater (Ólafsdóttir et al. 2002). The important role of water observed during the explosive phase is consistent with AVHRR and MODIS satellite

measurements of the high-altitude eruption cloud north of Iceland, revealing a strong ice or snow signal and a weak volcanic ash signal (Rose et al. 2001a, 2003). Ash fall was reported in the evening of 26 February, between 20:00 and 23:00, from ~ 100 km north of Hekla to the island of Grímsey off the northern coast of Iceland, ~ 300 km north from source (Haraldsson 2001). Individual lava streams were occasionally observed, when weather permitted, flowing down the northern, eastern, or southern flank of Hekla until 5 March and were reported to have stopped on 6 March.

Influence of the weather

To interpret the radar observations of the Hekla 2000 eruption cloud, it is important to analyse weather information spanning at least the explosive and lava fountain phases when coarse and fine tephtras were emitted and dispersed. Figure 5 shows rawinsonde measurements performed at the Keflavík synoptic meteorological station. Both radar (see next section) and satellite images (e.g. Rose et al. 2001a, 2003) illustrate the strong influence of the low systems around Iceland on both the proximal and long-range advection patterns of the Hekla 2000 eruption cloud. Continuous precipitation in north Iceland on the 26th and 27th and cold tropospheric temperatures also affected the composition of the advecting eruption cloud during the explosive and lava fountain phases, when coarse and fine tephtras were emitted and dispersed. Temperatures colder than -15°C are encountered at all levels higher than 2 km above sea level over Hekla in February (Fig. 5). As liquid water freezes on ash particles at those temperatures (e.g. Rose et al. 1995b), one must conclude that water vapour would have condensed quickly and nucleated ice coatings on ash early on in the subplinian phase. This is consistent with the indirect inference for ice encasing ash in the distal

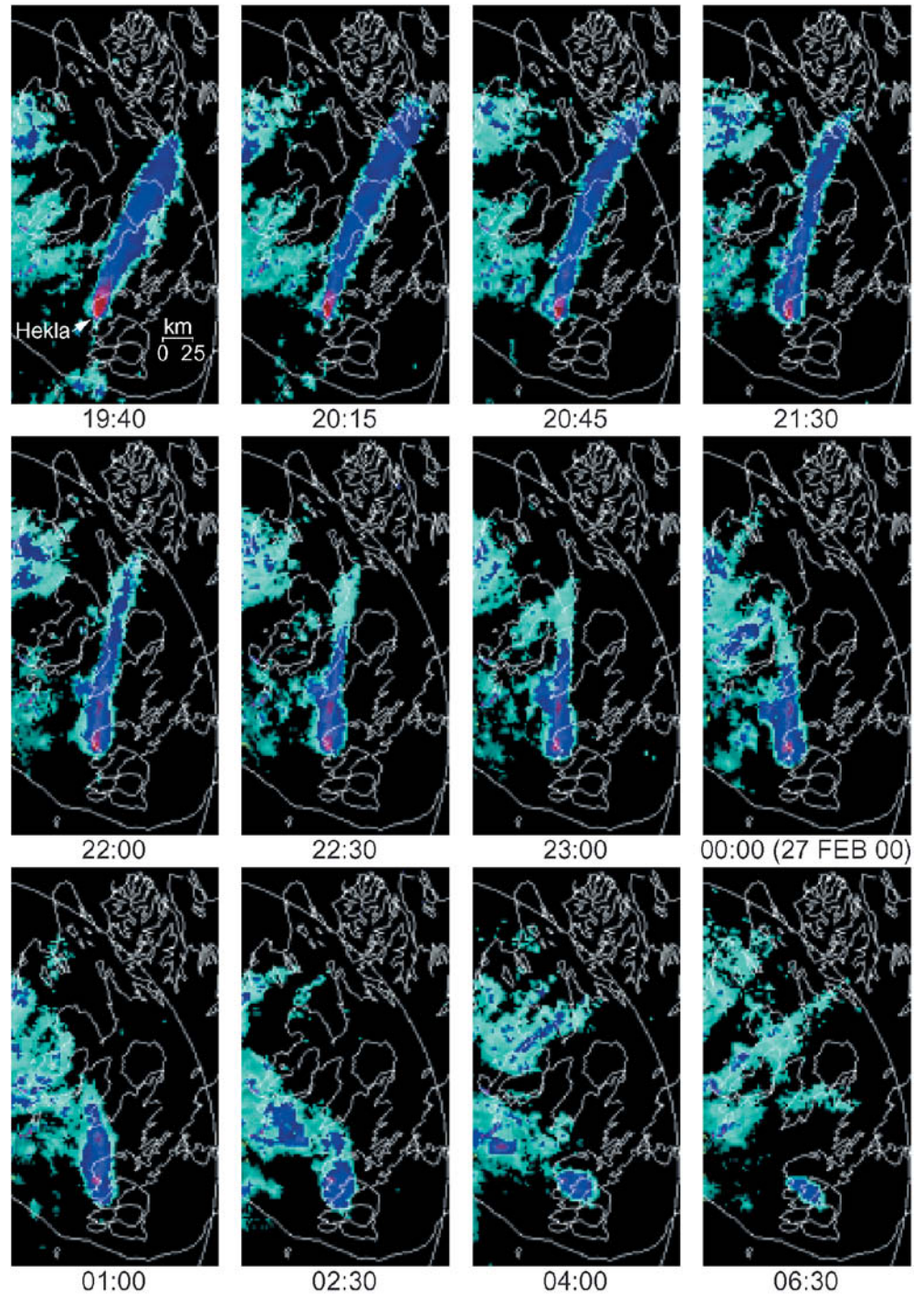
Fig. 6 Time series of selected VMI normal images covering the first 12 h of the Hekla 2000 eruption. Time (UTC) of each image relates to the starting time of the 2-min radar scan (see Fig. 3)



volcanic cloud made by Pieri et al. (2002). The expected effect is to cause a rapid change in the nature of the radar signal from one briefly dominated by ash reflection, followed by a drop in reflectivity (see Fig. 6) due to the fact that the radar reflectivity factor of ice is twice as low as that for ash (Adams et al. 1996). This reduction in radar reflectivity is somewhat mitigated, however, by an increase in reflectivity related to the larger size of ice- or snow-overgrown particles. Satellite studies also

showed that ice (or snow) very quickly formed on ash in the Hekla eruption column (Rose et al. 2003), in effect preventing the detection by IR satellite remote sensing of ash in the volcanic cloud. A similar effect was previously reported for the Rabaul 1994 volcanic cloud by Rose et al. (1995b).

Fig. 6 (continued)

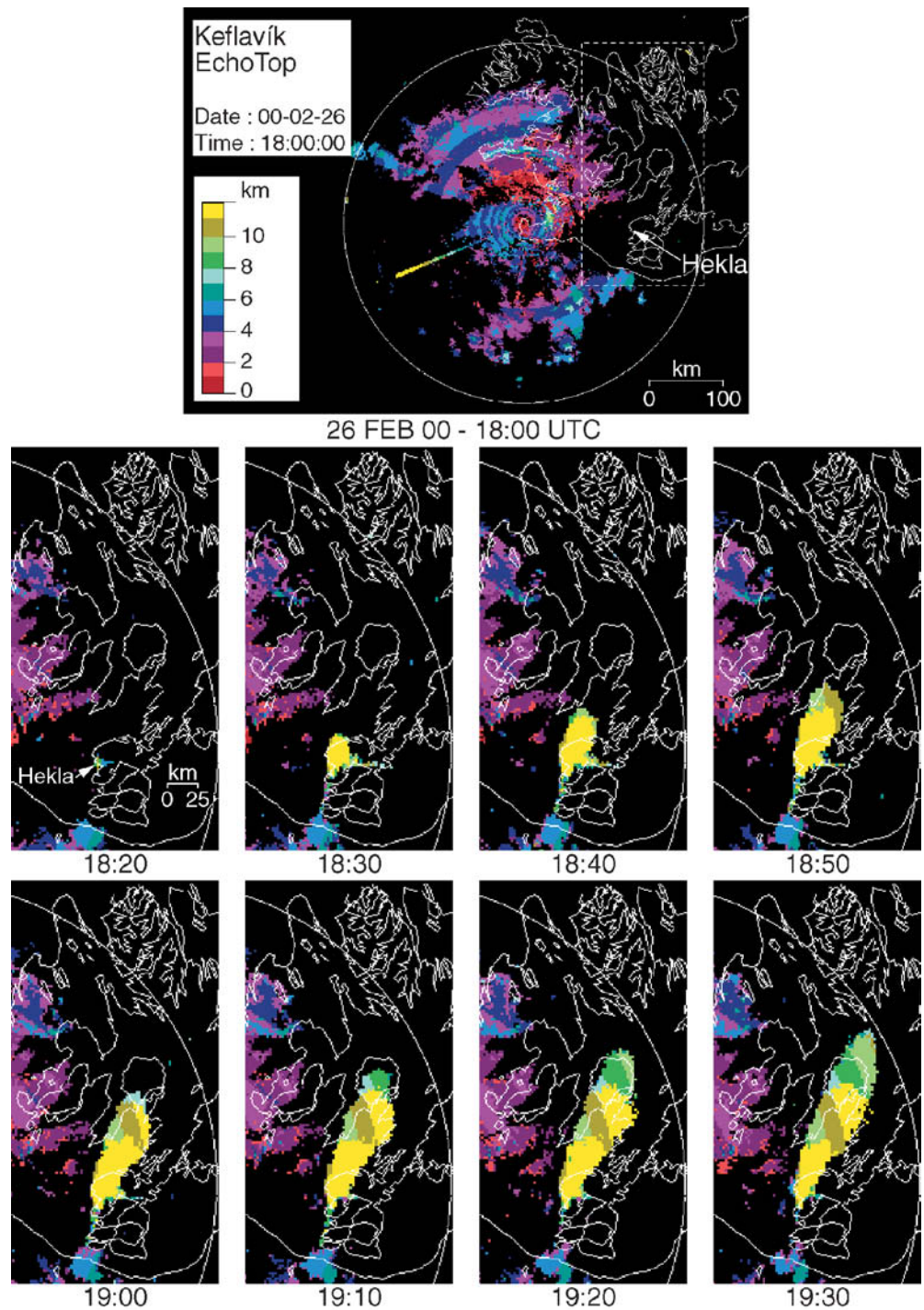


Real-time radar observations during the first 12 h of the eruption

Selected PPI images displayed by VMI normal and Echotop screens are shown in Figs. 6 and 7. The first radar echo of the Hekla 2000 eruption cloud was detected at 18:20 on 26 February. The echo is represented by a small region with strong reflectivity between 45 and 60 dBz, attributed to high initial column concentrations of ice- or snow-encased lapilli and coarse ash, and possible

large snowflakes containing ash (snowflakes containing ash were observed falling near Hekla at ~ 20:00–22:00; H. Mattson, personal communication, 2003). Taking into account the 2-min revolution of the radar antenna (Fig. 3), information from the corresponding Echotop image on Fig. 7 indicates that the head of the eruption column reached over 11–12 km height a.s.l., between the third (18:20) and fifth minute (18:22) after eruption onset (18:17). The mean ascent velocity of the plume head is

Fig. 7 Time series of selected Echotop images covering the first 12 h of the Hekla 2000 eruption. Concentric circles result from errors in pixel positions due to use of the nearest neighbour technique, when converting input data from polar co-ordinated to fixed position in Cartesian coordinates in the output image (Karlsson 1997)

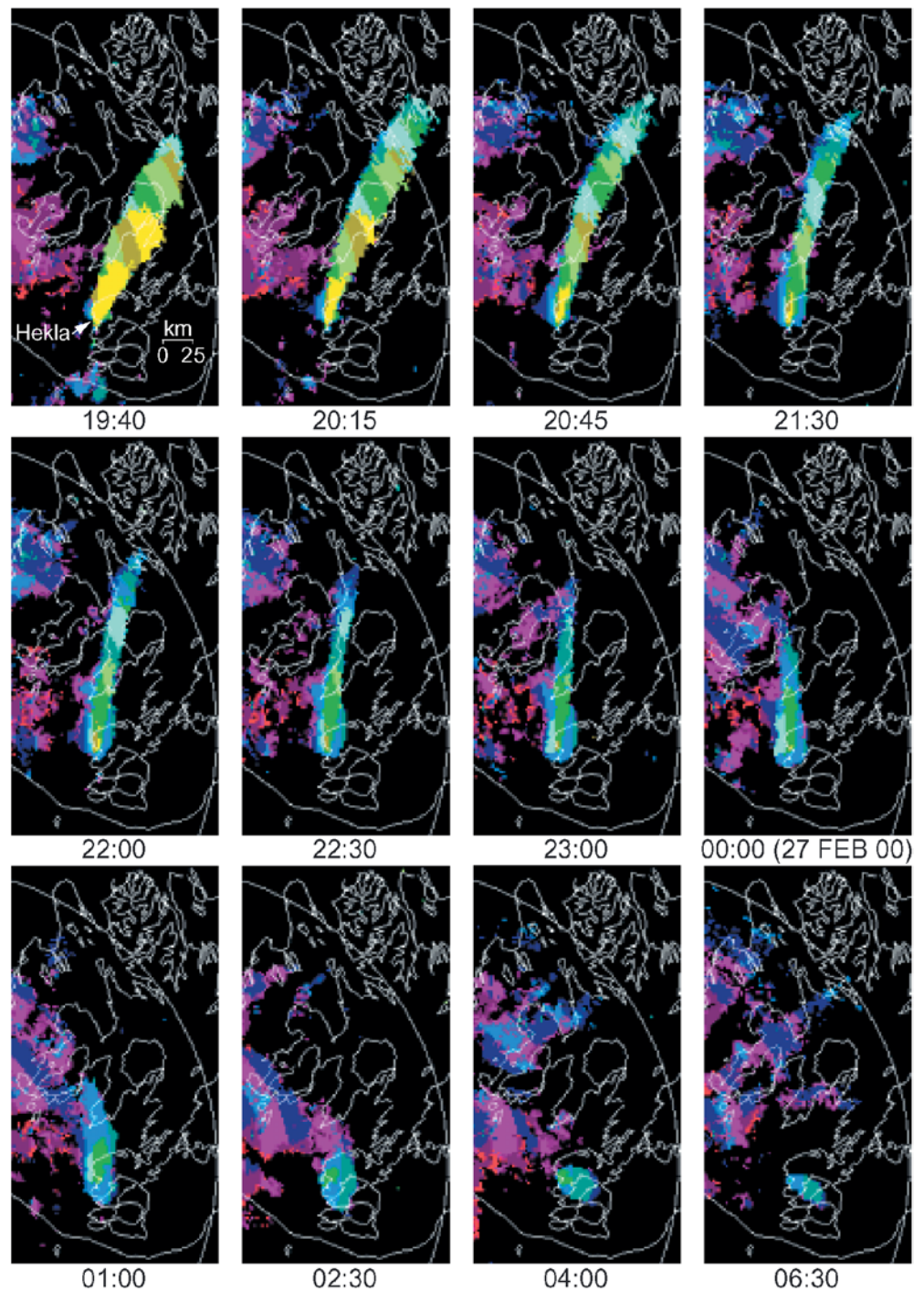


estimated to have ranged between ~ 30 and ~ 50 m s^{-1} during this early stage of the explosive phase.

A systematic documentation of the highly reflected plume during the first 12 h of the eruption is later presented and tied to the continuous volcanic tremor record (Soosalu et al. 2002; H. Soosalu, unpublished data, 2003). Figure 8 shows that the >45 -dBz portion of the emerging eruption column continues to grow crosswind and downwind until 18:50, with the highest echo of >60 dBz observed at 18:30 above Hekla. The highest

initial reflectivity is attributed to high concentration in the column of small ice- or snow-encased lapilli and coarse ash. Similar high radar return levels have been documented for the 1992 Spurr eruptions (Rose et al. 1995a), and corresponded to 2- to 20-mm particles there. An important difference was that the Hekla cloud produced a radar return for a considerably longer time and imaged area, of 2.5 h and over 300 km downwind distance, as opposed to 30 min and 20–30 km downwind distance for the Spurr cloud. We attribute this difference to the continuing

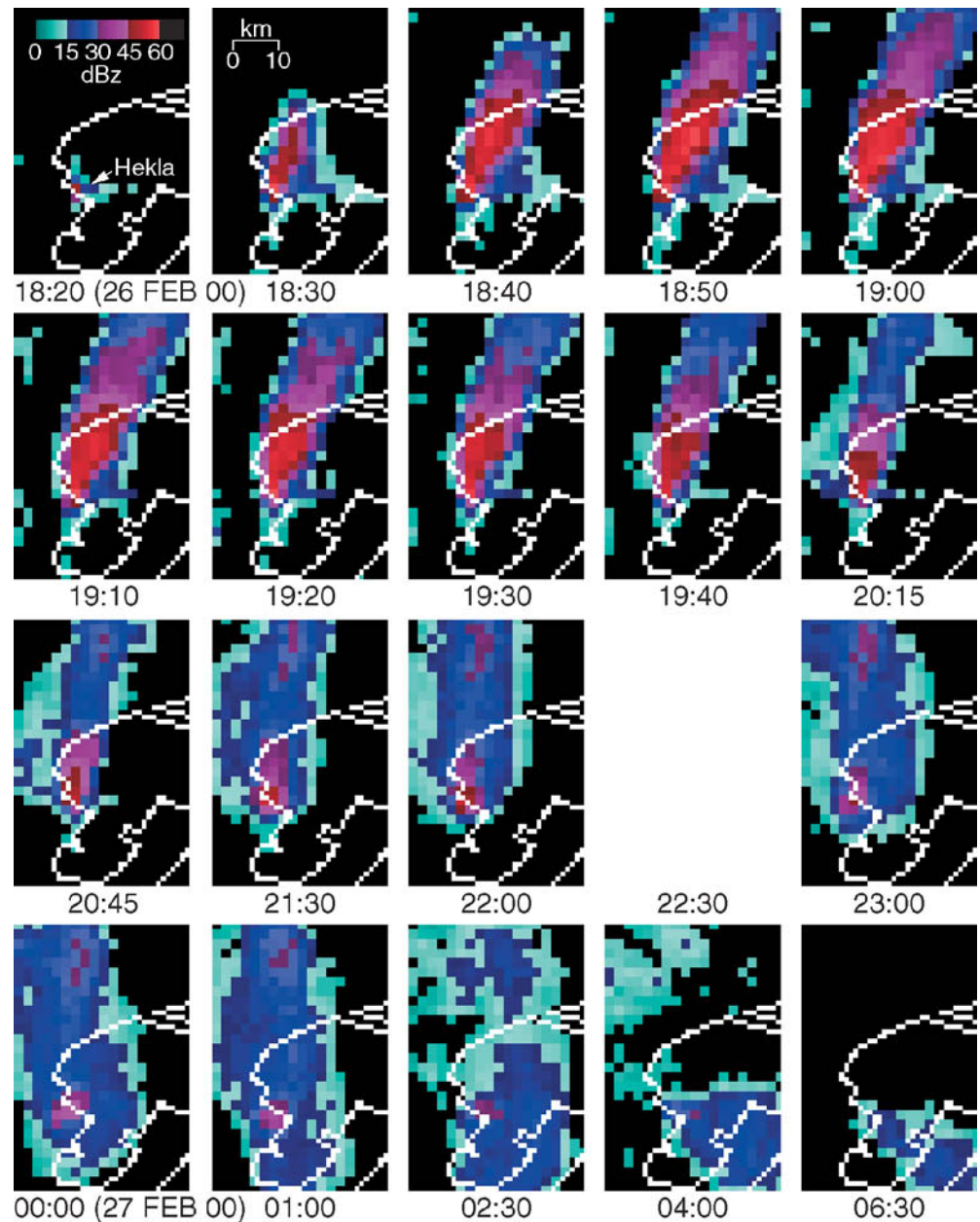
Fig. 7 (continued)



presence of abundant ice or snow encasing ash and the overgrowing of these mixed particles in the advected Hekla cloud. Surrounding the >30 -dBz reflected portion of the eruption column, an external envelope of low reflectivity, between 0 and 30 dBz, widened from 18:25 as the eruption cloud began to spread and to be advected in the lower stratosphere at an average speed of ~ 30 m s^{-1} to the north-northeast (Fig. 6). At 18:40 the cloud reached approximately $64^{\circ}20'N$, with its top height at ~ 11 – 12 km a.s.l. and its edges reaching up to ~ 9 – 10 km height a.s.l.

(Fig. 7), i.e. slightly above the tropopause. At 19:00 the reflected cloud edge at 0–15 dBz reached the southern margin of Hofsjökull glacier and slightly dropped to an elevation of ~ 7 – 8 km (Figs. 6 and 7). As the eruption cloud advected over the glacier, it became asymmetrical with a secondary lobe of low reflectivity at 0–30 dBz, developing on its eastern side. The secondary lobe did not progress farther than the southern ice margin of Hofsjökull and reached its maximum lateral extent between 19:15 and 19:25 based on the analysis of the whole radar

Fig. 8 Time series of selected Cappi level 2 images showing evolution of the highly reflected portion of the eruption column during the first 12 h of the Hekla 2000 eruption. Image not available at 22:30



data set. At the same time, the main cloud continued to be advected at a near-constant speed of $\sim 30 \text{ m s}^{-1}$ towards the north-northeast along a $\sim \text{N}20^\circ\text{E}$ azimuth, to reach Saurbaer in Eyjafjörður at 19:45, $\sim 65^\circ 30'\text{N}$ and $18^\circ 15'\text{W}$ (Figs. 2 and 6). However, a spot reflecting 15–30 dBz and reaching $\sim 10 \text{ km}$ height a.s.l. was located east of Hrísey in Eyjafjörður, $\sim 66^\circ\text{N}$ and $18^\circ 15'\text{W}$. This may indicate that a portion of the cloud advecting in lower-level winds reached $\sim 66^\circ\text{N}$ at this time but at an altitude generally below the radar detection limit at this location, i.e. below 7–8 km height a.s.l. (Fig. 2). At 20:05 another spot was seen farther north than the main eruption cloud at $\sim 65^\circ 50'\text{N}$ and $17^\circ 40'\text{W}$, reflecting at 15–30 dBz and reaching 8–9 km height a.s.l. It is unlikely that these radar-detected spots were from precipitation clouds even

though it was snowing at this time in northern Iceland. The Echotop images on Fig. 7 show that, in a 200-km radius from the radar, the top of precipitation clouds did not exceed 3–5 km height a.s.l. overall. Thus, once again, these spots may correspond with the radar detecting some ash at the edge of its height range.

By investigating the radar images thoroughly there are more indications that the outer limit of the eruption cloud was wider than generally seen in Fig. 6. For instance, at 20:20 a reflected spot was seen west of the main flow and east of it at 21:00. This is in good agreement with the maximum extent of the eruption cloud observed by the MODIS sensor at 21:00 [see Fig. 2 in Rose et al. (2003)]. A limitation of the radar data is illustrated by comparing the data with the MODIS satellite image. The MODIS

image displays a bifurcation pattern in the extreme northeast of Iceland that is not at all apparent on the radar image for that time and location, most likely because bifurcation becomes more apparent beyond the Keflavík radar range.

A key pattern of the eruption cloud, reflected by the radar, is that the strongest reflection is seen during the early eruption stage, i.e. approximately during the first 90 min (Fig. 6). This correlates very closely with the phase of fastest increase in total mass retrieved by IR satellite sensors (Rose et al. 2003). After that, the maximum echo of >30 dBz is only seen over the vent and just north of it. Despite this, an increase in the reflection is observed north of the vent at ~64°20'N and 19°30'W. The spot is clearly seen between 20:35 and 01:00 on 27 February and the reflection is >30 dBz, while in the surroundings it reflected at 15–30 dBz (Figs. 6 and 8). The possible origin of this second highly reflective portion of the eruption cloud is later discussed and related to mixed-phase aggregation, i.e. between ice-encased or snowflake-encased ash particles (see Textor et al. 2003a, 2003b). From about 20:30 the azimuth of the advecting eruption cloud gradually shifted towards the north-northwest as a result of change in wind direction (Figs. 5 and 6). By 21:00 the reflected cloud covered only the western part of Hofsjökull glacier. Its extent diminished and 1 h later its northern limit is seen west of Hofsjökull glacier at ~65°20'N. At 01:00 the eruption cloud only reached 64°20'N along a ~N10°E azimuth (Fig. 6). Volcanic activity continued to decrease and 12 h after its start there was only seen reflection above the vent and east and east-southeast of it (Figs. 6 and 8). Cloud height was between 5 and 7 km a.s.l. at this time (Fig. 7). This corresponds closely to the time when the total mass of particles retrieved by IR satellite sensors started to plunge (Rose et al. 2003).

Volcanic tremor and evolution of the reflected plume and proximal fallout

Hekla volcano is located at the eastern tip of the South Iceland Seismic Zone (SISZ). The earthquake activity of this region has been continuously monitored since 1990 after a network of seismograph stations was installed by IMO in 1988 (Stefánsson et al. 1993). The South Iceland Lowland (SIL) project was originally aimed at recording the magnitude and the location of earthquakes occurring along the SISZ. The 1991 Hekla eruption showed that the use of the SIL network of seismograph stations can be extended, beyond the normal recording of earthquake activity, to study the intensity and amplitude of volcanic tremor in different frequency bands (Soosalu and Einarsson 2002; Soosalu et al. 2003). The same investigation was repeated during the Hekla 2000 eruption (Soosalu et al. 2002; H. Soosalu, unpublished data, 2003). Out of the three operational seismograph stations used in the Hekla 2000 study, the Haukadalur station (HAU) is the nearest, only 14 km from Hekla, and recorded the highest

amplitude of volcanic tremor during the eruption (Fig. 9b). The simultaneous variations of the volcanic tremor amplitude and the reflected cross-sectional area of the eruption column and proximal fallout region show that both the seismic and radar signals are related to the same overall magmatic process occurring from the magma chamber to the open vent of Hekla. Both the tremor amplitudes and the denser portion of >45 dBz reach their maximum at ~18:50 before beginning to decrease. Tremor amplitudes continued to gradually decrease until 7 March, to reach similar values as those measured prior to the start of the eruption (H. Soosalu, unpublished data, 2003).

The volcanic tremor amplitude is found to increase with increasing plume height according to the empirical relation (Eq. 4) (McNutt 1994a, 1994b; McNutt et al. 1995).

$$\log_{10} \left(\frac{A\sqrt{\lambda r}}{2\sqrt{2M}} \right) = 1.80 \log_{10}(H) - 0.08, \quad \text{e.g. for surface waves} \quad (4)$$

where A is amplitude (cm) peak-to-peak; λ is wavelength (cm); r is distance (cm) from source to seismic station; M is seismograph magnification at the tremor frequency; and H is eruption column height (km).

An estimate of the magma mass discharge rate can be inferred from the maximum eruption column height using the Morton et al. (1956) equation (Eq. 5) (e.g. Carey and Bursik 2000):

$$H_t = 1.67Q^{0.259} \quad (5)$$

where H_t is maximum eruption column height (km) and Q is magma volume discharge rate ($\text{m}^3 \text{s}^{-1}$) of magma.

Equations (4) and (5) indicate that the recorded tremor amplitude and the volume discharge rate of magma can be linked empirically.

From PPI radar images intersecting the Hekla 2000 eruption column at the lowest possible detection height of ~2 km a.s.l. (i.e. Capi level 2), ~500 m above the 1,491-m-high vent, >30-dBz portions are thought to reflect the cross-sectional area of both the eruption column and proximal fallout region. Their area variation can be used as a rough indicator of the change in magma discharge rate (Fig. 8). As already described, the 30- to 45-dBz and >45-dBz portions are characterised by their short appearance and limited extent above the vent. The areas of the two highly reflected portions fluctuate over time, with a sharp increase from 18:20 until ~19:00 when they cover a maximum total area of 107 pixels or ~428 km² (Fig. 9a). The trough observed at 18:55 is interpreted to result from a defect in the reflected radar signal which affects the whole image. From ~19:00 the total area of the 30- to 45-dBz and >45-dBz portions (i.e. >30-dBz portion) rapidly decreases to about 30% of the maximum extent at ~19:20, only 1 h after the eruption onset, illustrating a rapid waning of tephra emission and fallout near the vent or more probably that the ash in the column even at this low

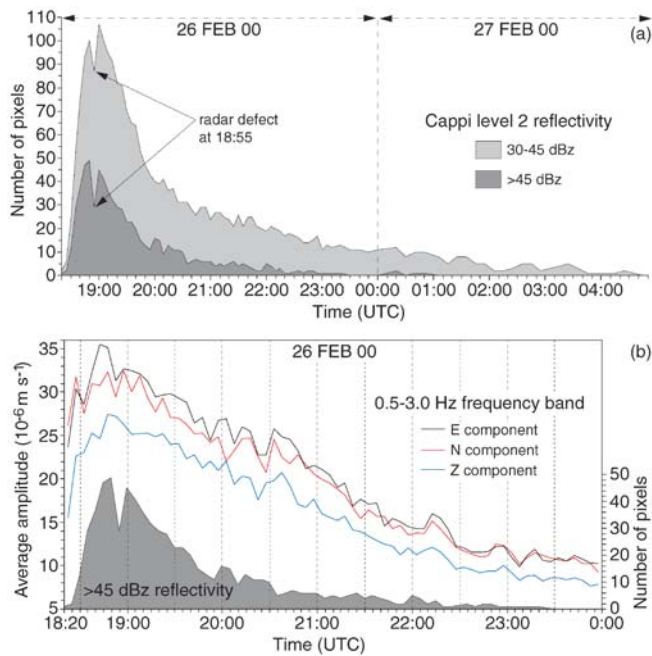


Fig. 9 **a** Evolution of the highly reflected portions of the eruption column during the first 10 h of the Hekla 2000 eruption, with the >45 and 30–45 dBz reflectivity fields (Cappi level 2) represented as *stacked areas*. **b** Variations of the >45 dBz reflectivity (Cappi level 2) of the Hekla eruption column and the 5-min average amplitude of tremor recorded at Haukadalur seismograph station (H. Soosalu, unpublished data, 2003)

elevation becomes increasingly hidden by ice or snowflakes nucleating and growing on the ash particles. From ~01:00 on 27 February, the >45-dBz portion completely disappears while the 30- to 45-dBz signal lasts until ~04:30.

Reflected cloud and ground-based observations of tephra fall

The reflected wind-advected cloud of the Hekla 2000 eruption can be compared with the associated tephra fallout on the ground, from both eyewitness accounts and study of the primary deposit (Fig. 10). The onset of tephra fall, as the eruption cloud advected to the north-northeast of Hekla towards the island of Grímsey, off the northern coast of Iceland, was recorded at several localities. From ~20:00 until 23:00, tephra fall was reported from the northern margin of Hofsjökull glacier to the island of Grímsey, ~120 and ~300 km downwind from Hekla, respectively (Fig. 10b). Rough estimates of ash modal size at these two locations are ~200 and ~63 μm , respectively (Haraldsson 2001; G. Larsen, unpublished data, 2003). The size distribution of ash fall contains a coarse tail of larger particles which are the ones that dominate the radar return. The mean speed of the advancing fallout front is estimated to ~18 m s^{-1} along a main ~N10°E azimuth. The timing and direction of the

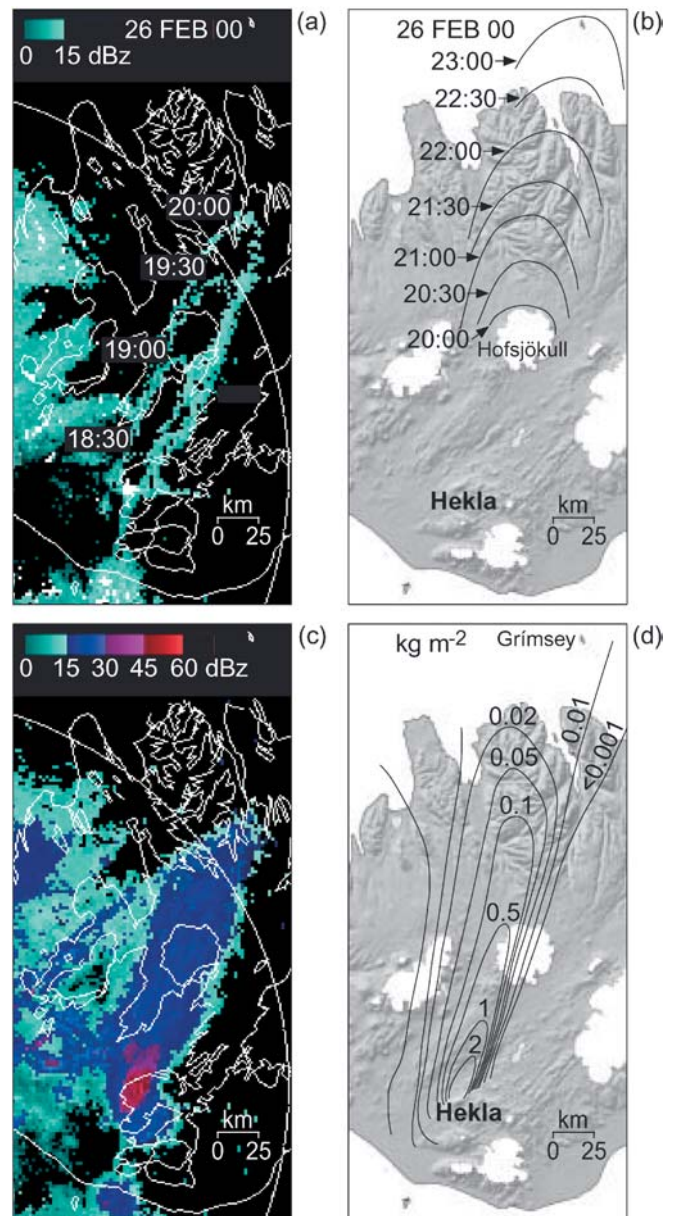


Fig. 10 **a** Advancing edge of the 0–15 dBz reflected Hekla 2000 eruption cloud (VMI normal). **b** Ground-based observation of the onset of the Hekla 2000 tephra fall (Haraldsson 2001). **c** Composite reflectivity (VMI normal) of the Hekla 2000 eruption cloud for the first 12 h. **d** Isomass map of the Hekla 2000 tephra fall (Haraldsson 2001; G. Larsen, unpublished data, 2003)

advancing fallout front differs from that of the observed reflected advecting cloud on VMI normal images (Fig. 10). PPI images indicate an early advection direction to the north-northeast from ~18:20, shifting towards a north direction at ~23:00 (Fig. 6). The radar detection height exceeds 7 km a.s.l. at 280 km from the antenna (Fig. 2b). Any portion of the advected ash cloud below this height cannot be detected by the radar beam, i.e. north of the southern part of Eyjafjörður (Fig. 2a). The lack of any significant radar signal beyond this range indicates that most of the ash cloud already drifts below

an elevation of 7 km over Eyjafjörður and the island of Grímsey. South of this detection range, the advancing 0- to 15-dBz front of the reflected plume can be mapped at regular time intervals in a similar manner as for the onset of tephra fall (Fig. 10a). This indicates that the reflected front of the advected cloud front precedes the onset of tephra fall by about 30 min at the northern margin of Hofsjökull, and by about 2 h just south of Eyjafjörður, indicating that tephra mainly fell out from the eruption column and was advected to the ground by lower-level winds (Lacasse 2001). It is assumed that most of the tephra fell within the first 12 h, covering an area of ~18,000 km² (Haraldsson et al. 2002). In order to compare the radar observation with the distribution and characteristic of the primary tephra fall deposit on snow [i.e. in terms of mass loading or thickness (Haraldsson 2001; G. Larsen, unpublished data, 2003)], a map of the composite reflectivity is reconstructed by integrating all the VMI normal snapshots from Fig. 6 (Fig. 10c). The composite reflected cloud is oriented along an ~N25°E azimuth and entirely overshadows the Hofsjökull glacier. In comparison, the isomass contours indicate that tephra deposition occurred along an ~N15°E azimuth and only affected the western half of Hofsjökull as shown by the <0.001-kg m⁻² outermost envelope (Fig. 10d). This reflects the observation made earlier on the azimuth change of the low-level winds into which falling particles are advected on their way to the ground as well as the azimuth change of the reflected cloud axis and resulting ash dispersal over time (Fig. 6). Differences between the radar- and ground-based observations of ash dispersal most likely result from the more easterly and northerly directions of the lower-level winds on the evening of 26 February. They are consistent with the fact that the greater part of the on-land fall deposit in Iceland is from particles falling off the column margins and advected to the ground by lower-level winds (e.g. Ernst 1997; Lacasse 2001).

Discussion

Particle size and concentration within the reflected volcanic cloud

With RHI images available, the height of the volcanic cloud can be determined together with the signal decrease with time due to gravitational settling of coarse particles (Harris et al. 1981; Harris and Rose 1983; Rose et al. 1995a). This only works provided that a sufficient number of large particles is kept in the column and carried all the way to its very top, as experimentally and theoretically supported by Ernst et al. (1996). Harris and Rose (1983) estimated the size of the falling tephra from the 19 March 1982 Mount St. Helens eruption, by looking at the RHI reflected top of the eruption cloud at different times as it advects downwind, assuming no vertical air motion. The latter assumption is reasonable for relatively weak eruption columns such as the 1982 Mount St. Helens eruption (Harris and Rose 1983) and most likely during

the 2000 Hekla eruption. The initial decrease in elevation of the reflected cloud top, after the eruption column reached its maximum elevation, is thought to mainly result from settling of the coarsest particles with few small ones that are scavenged. As shown by the Probert-Jones' (1962) equation (Eq. 6), the radar echo, or received reflected power P_r , from a radar target composed of randomly distributed targets, i.e. ice, snow, or small lapilli and coarse ash in this case, is mainly controlled by their particle size or, for a given modal size, by their concentration (number density) in the cloud:

$$P_r = \frac{\pi^3}{16 \ln 2} \frac{P_o h G^2 \theta \phi}{\lambda^2 R^2} \left| \frac{\epsilon - 1}{\epsilon + 2} \right|^2 \sum r^6 \quad (6)$$

where P_r is received power (kW); P_o is peak transmitted power (kW); h is radar pulse length (km) in space; G is actual gain of antenna (dB); θ is horizontal beam width (degrees) to the -3-dB level for one-way transmission; ϕ is vertical beam width (degrees) to the -3-dB level for one-way transmission; ϵ is dielectric constant of spherical particles; λ is wavelength (cm); R is range or distance (km) to the target; and r is radius (mm) of spherical particles.

With the return radar signal dominated by the largest most abundant particles suspended in the cloud, their terminal settling velocities can be calculated by measuring the initial decrease in height of the most highly reflected portion of the cloud on RHI images. Particle sizes in the cloud can then be estimated from the apparent settling velocities, e.g. in the order of 300 cm s⁻¹ about 20 min after the 1982 Mount St. Helens eruption column reached its maximum height (Harris and Rose 1983). Using an empirical relationship between terminal settling velocity, diameter, density of spherical tephra, and altitude (e.g. Wilson 1972), the particle sizes were inferred, suggesting a mean 250- μ m diameter in the case of vesicular tephra and plagioclase crystal of 2.5 g cm⁻³ bulk density. Similarly, smaller particles, ~180 μ m in diameter, were inferred from the slower height decrease of the plume top, ~170 cm s⁻¹, later during the course of the eruption. The lower and upper bounds for the ash concentrations of the 1982 Mount St. Helens cloud were also estimated, e.g. between 0.2 and 0.6 g m⁻³ for particles larger than 180 μ m (Harris and Rose 1983). In comparison and from ground-based observation alone, the grain size of the Hekla 2000 tephra fall decreases rapidly along the axis of thickness, from a mean of 4.3 mm (~-2.12 phi unit) at 11 km from source (Hekla summit) to 204 μ m (~-2.29 phi unit) at 80 km and 165 μ m (~-2.60 phi unit) at 170 km. Corresponding sorting values decrease from 1.95 to 0.89 and 0.80, respectively, whereas maximum grain size decreases from 45 mm (fragments, largest bomb 96 mm) to 2 mm, and 0.8 mm (Árnason 2002; G. Larsen, unpublished data, 2003).

Effects of water phase, particle size, and silica content on the reflected signal

The height of the advecting Hekla 2000 eruption cloud cannot be accurately monitored by the radar as in the 1982 Mount St. Helens case due to the unavailability of RHI vertical radar profiles. Therefore, particle sizes and concentrations within the reflected Hekla cloud cannot be inferred using the Harris and Rose (1983) procedure. Ash aggregates and ice- or snow-coated ash particles due to the large amount of water in the plume would make such estimate most likely inconclusive in any case. The high water content of the 2000 Hekla cloud has at least four possible origins: (1) the dissolved water content in the magma prior to eruption, (2) magmatic water which has been derived from crystallization of stored magma under the volcano and which is then trapped by a hydrothermal cap or some other means until eruption (Giggenbach et al. 1990), (3) the presence of groundwater within the volcano edifice (Ólafsdóttir et al. 2002), and (4) entrained ambient atmospheric humidity and resulting precipitation (e.g. snow). Ice or snow most likely began to form early within the eruption column itself once its temperature equilibrated to the ambient freezing temperature (Fig. 5). The mean reflectivity factor K for volcanic ash is 0.39, 2.4 times less than liquid water droplets (0.93) and two times more than ice (0.197) for the same particle size and radar wavelength (Rose and Kostinski 1994; Adams et al. 1996). The VMI normal images integrate the maximum reflectivity measured from ~2 to ~12 km height a.s.l. across the rising column and advected cloud (Fig. 3). However, the reflected signal from larger particles is dominant by far over effects of the reflectivity factor. Thus the sustained duration and larger extent of cloud reflectivity and the secondary maxima detected most likely are due to continuing growth of ice (or snow) around ash particles in the advecting cloud. We suggest that the >30-dBz portions of the eruption column itself observed above the vent and its vicinity (Fig. 8) mainly reflect high abundance of small lapilli (5–20 mm in size) and coarse ash (hundreds of microns in size) encased by ice, and large unmelted snowflakes that nucleated on ash [likely size, 2–20 mm; Graedel and Crutzen (1993)]. Reflectivity between 0 and 30 dBz observed in the advected cloud and fallout zone in the eruption column wake is mainly consistent with lower particle concentrations there compared to the column core, and with the smaller sizes of ice- or snow-coated particles undergoing partial melting or sublimation [100 μm to 2 mm in size; Graedel and Crutzen (1993); Fig. 6]. The influence of the small composition range of tephra, from basaltic andesite to dacite, on the reflected signal can be considered as insignificant (Adams et al. 1996).

A second >30-dBz portion of the advecting cloud can be observed ~30 km north of Hekla volcano on the VMI normal and Capi level 2 images, from ~20:45 on the 26th until ~01:00 on the 27th February (Figs. 6 and 8). Its maximum extent is ~60 km² at 22:25. Both the extended signal for the Hekla cloud for about 2.5 h [i.e. five times

longer than for the Spurr cloud; Rose et al. (1995a)] and its second reflective portion suggest a possible increase in the diameter of the suspended particles due to growth of hydrometeors and/or buildup of ice/ash aggregates (Textor et al. 2003a, 2003b). Due to the lack of field data, the extent of aggregation cannot be matched with the possible development of secondary ash accumulation on the ground. Study of the radar data set for the Hekla 1991 eruption cloud shows a second high-reflectivity portion within the advecting cloud on VMI normal images, from the same region extending farther north to the southern margin of Hofsjökull glacier, with no apparent secondary thickening observed for the associated tephra fall deposit (Larsen et al. 1992). Similar radar observations were made by Harris et al. (1981) for the 18 May 1980 eruption of Mount St. Helens, but in that case secondary downwind deposit thickening was observed (Carey and Sigurdsson 1982). Both the 1991 and 2000 radar observations, made under similar weather conditions and above the same region, are consistent with enhanced ice or snow particle growth in the advected cloud, following the large release of magmatic or hydrothermal water suggested by Rose et al. (2003).

Potential use and limitations of weather radar for eruption cloud tracking

Although the weather radar we used is designed to monitor precipitation clouds and not specifically designed for volcanological use, as, for example, the NEXRAD system developed in the Cook Inlet volcanic region of Alaska (e.g. see Krohn et al. 1995; Rose et al. 2001b), we demonstrated that the Keflavík radar can also be used to locate and track volcanic clouds over the Iceland region. Near-real-time monitoring of volcanic clouds can be achieved and provides invaluable information for relevant meteorological centres and aviation authorities [e.g. Icelandic Civil Aviation Administration (CAA), Air Traffic Control Centres, and London, Toulouse, and Montreal Volcanic Ash Advisory Centres (VAAC)] that are concerned with preventing encounters of aircrafts with volcanic clouds. For volcanoes like Hekla, located within 150 km of the radar, eruption column rise can theoretically be detected within a few minutes of eruption onset, thereby providing one of the most crucial pieces of information for forecasting models: the eruption onset time. The eruption clouds can be tracked from some hundreds of meters above the volcano up to the current 12-km elevation limit imposed by the existing radar software system. The real-time observation of the Hekla 2000 eruption is an optimum case in Iceland for the volcanological application of the present radar configuration. The eruption column above the vent and associated ash cloud advected to the north-northeast were almost completely and continuously detected. Both phases of the rising eruption column and advecting cloud have been monitored from the time series analyses of PPI (plan-position indicator) radar images that included VMI

normal, Capi level 2, and Echotop displays. From the reflectivity values of the first two modes of data output, the relative role of ash and water phases in the volcanic cloud can be assessed on a qualitative basis by checking them against ground-based observations of the ash fall deposit.

In the case of the Hekla 2000 eruption, values of >30 dBz can be essentially accounted for in terms of radar reflectivity returns dominated by high concentrations in the column itself of small lapilli (expected modal size of ~ 0.5 – 5 mm based on fall data), and possibly including coarse ash particles encased in ice or snow (ice-coated particles of up to 0.5 – 2 mm), and large unmelted snowflakes [expected size up to 5 – 20 mm; Graedel and Crutzen 1993; Houze 1993] or snowflake aggregates containing ash. Radar return values between 0 and 30 dBz for regions of the cloud with longer atmospheric residence (0.5 – 3 h) are explained as the result of hydrometeors and/or aggregates which are also the size of small lapilli but less numerous than the particles in the eruption column due to fallout, with the hydrometeor size decreasing as a result of partial melting and/or sublimation. Secondary increases in reflectivity downwind from vent in the Hekla cloud, which, for example, were also well documented in the 18 May 1980 Mount St. Helens cloud (Harris et al. 1981), are most easily accounted for in terms of increase in effective particle size originating from mixed phase aggregation taking place in the volcanic cloud (see Textor et al. 2003a, 2003b).

As shown by Eqs. (4) and (5), an empirical relation can be established between the evolution of the highly reflected portion of the eruption column, >30 dBz, and the variation of the volcanic tremor amplitude, both reflecting the change in tephra emission or magma discharge rate during the course of the explosive phase of the eruption. The time series analysis of the reflected Hekla eruption cloud as it drifted away from source shows some differences with the timing and distribution of ash fall deposition due to the influence of winds in the lower troposphere and the boundary layer above the ground. In the absence of RHI (range-height indicator) images and despite some errors in the pixel positions, the Echotop images are, to date, the primordial source of information on the height variation of the ascending eruption column head and the advecting eruption cloud.

In the light of the detection limits just outlined and of the growing volume of air traffic in the region, there is an urgent need to upgrade the Keflavík radar system for both meteorological and volcanological monitoring. As Fig. 2 clearly shows, a radar at a fixed location can only monitor a limited number of active volcanic systems in Iceland, i.e. those located within 150 km of Keflavík: Hekla, Tindfjallajökull, Eyjafjallajökull, and Vestmannaeyjar (Heimaey). Several of these volcanoes are potential sources of subplinian and plinian eruption columns and advected clouds much higher than 12 km altitude. In 1947 Hekla produced an eruption cloud initially rising to 30 km elevation (Thórarinnsson 1954). If such an eruption occurs today, the Keflavík radar would detect less than half of its

column (Fig. 2). The current upper detection limit of 12 km for the Keflavík radar prevents any tracking of these future eruption columns and is therefore inadequate for aircraft safety use. Eruption plumes from volcanoes located at least 250 km farther east, i.e. Grímsvötn, Öraefajökull, Askja, and Krafla, will also not be adequately detected by the radar (Fig. 2). The retrieval of RHI images in addition to PPI images up to at least 20 km height a.s.l. must be made achievable as soon as possible. Seismic unrest and inflation of the caldera of Katla volcano (Mýrdalsjökull glacier), at a distance of ~ 180 km from the radar (Fig. 2), are ongoing and becoming a major concern for volcanic hazard in Iceland as this volcano is known to have generated major subglacial and explosive eruptions in the past, e.g. the Katla 1918 eruption with a recorded eruption column height of at least 14 km (Larsen 2000) and sometimes columns reaching up to 20 – 30 km elevation (e.g. Lacasse et al. 2002). In this particular scenario, the Keflavík radar would detect less than half of the Katla eruption column (Fig. 2). A major fissure eruption such as the 1783–1784 Laki eruption, which had perhaps the most severe atmospheric effects of all Icelandic eruptions (Thórdarson and Self 2003), would be at the limit of the radar range.

Conclusion

In this paper the first 12 h of development of the Hekla 2000 eruption cloud have been described. The data set and analysis closely complements in-situ sampling data from a brief encounter with the distal Hekla cloud as reported by Pieri et al. (2002) and the integrated multi-sensor satellite study of the same cloud by Rose et al. (2003). We have focused here on the information retrieved from the only weather radar operated by the Icelandic Meteorological Office (IMO). We illustrated that the radar can be used, in addition to monitoring precipitation clouds, to locate and track volcanic clouds in near-real-time over Iceland. The radar proves to be one of the most valuable and cost-effective tools for the meteorological agencies and aviation authorities in terms of preventing encounters of hazardous volcanic particles with aircrafts. From this study and the work of Rose et al. (2003), the Hekla 2000 volcanic cloud is the most closely documented to date by radar and satellite remote sensing, with the added benefit of a considerable wealth of geophysical, meteorological, and field deposit observations. The results are now available for testing of theoretical models on the dynamics of volcanic clouds and ash fallout.

Currently, there are also undesirable limitations in the existing radar software system limiting the monitoring capability of tracking volcanic clouds. The maximum height displayed is only 12 km a.s.l. and the RHI images are not available. Considering future eruptions in Iceland and the growing volume of air traffic in the Icelandic Oceanic Control Area over the North Atlantic-Arctic region, an upgrade of the radar software system is most

urgent. IMO is currently working towards upgrading the radar software, which will be operational by early spring 2004. The new software will be more flexible, i.e. all available information that can be retrieved by the current radar will be accessible and there will be no restriction in the vertical. More accurate information on eruption cloud heights and their near-real-time change will become available. This information is one of the most crucial for aviation safety and provides a near-real-time input of relevant data for trajectory and dispersion models expected to lead to improved forecasts of ash dispersal. RHI images will also be available, providing crucial information (e.g. vertical cross section) on the initial development and vertical distribution of erupted material in the eruption column and advected cloud generated from it. RHI data will enable some estimation of the effective grain size distribution of falling material. Despite these planned improvements, others are also needed. Due to its fixed location, the radar covers only the western half of Iceland. For full coverage three additional radars are needed to encompass the eastern, northern, and southern flight sectors over Iceland. This will not only improve the monitoring of volcanic clouds but most importantly be very valuable for daily meteorological use over Iceland and its surroundings, by providing invaluable information for air traffic safety related to non-volcanic hazards (e.g. icing condition, air turbulence). Some of these efforts, as well as volcanological monitoring and studies, would greatly benefit from more sophisticated radar systems including higher beam resolution (e.g. NEXRAD), Doppler-shift capabilities, and polarization retrievals (e.g. see Houze 1993).

Acknowledgements The authors would like to thank the Icelandic Meteorological Office and the Science Institute at the University of Iceland for their support, and especially Philippe Crochet, Hreinn Hjartarson, Hrafn Gudmundsson, Erik Sturkell, Kjartan Haraldsson, and Stefán Árnason for fruitful discussions and for giving access to unpublished data. The Icelandic Civil Aviation Administration provided very constructive comments throughout the study. C.L.'s research work was supported by internal funds from the Open University. G.G.J.E. acknowledges the support of the Fondation Belge de la Vocation, the Belgian NSF (FWO-Vlaanderen), and Ghent colleagues. Peter Mouginiis-Mark, David Pieri, and an anonymous reviewer are acknowledged for thorough reviews of the manuscript.

References

- Adams RJ, Perger WF, Rose WI, Kostinski A (1996) Measurements of the complex dielectric constant of volcanic ash from 4 to 19 GHz. *J Geophys Res* 101:8175–8185
- Ágústsson K, Stefánsson R, Linde AT, Einarsson P, Sacks IS, Gudmundsson GB, Thorbjarnardóttir B (2000) Successful prediction and warning of the 2000 eruption of Hekla based on seismicity and strain changes. In: Proc AGU 2000 Fall Meeting, *Eos* 81, F1337, Abstract.
- Árnason SG (2002) Heklugosid 2000: Kornastaerd, berggerd og kornalögun gjóskunnar (in Icelandic) (The Hekla 2000 eruption: grain size, composition and shape of ash particles). BSc Thesis, University of Iceland, 81 pp
- Cantor R (1998) Complete avoidance of volcanic ash is the only procedure that guarantees flight safety. *ICAO J* 53:18–19
- Carey SN, Bursik M (2000) Volcanic plumes. In: Sigurdsson H, Houghton B, McNutt S, Rymer H, Stix J (eds) *Encyclopedia of volcanoes*. Academic Press, San Diego, pp 527–544
- Carey SN, Sigurdsson H (1982) Transport and deposition of distal tephra from the May 18, 1980 Mount St. Helens. *J Geophys Res*: 87:7061–7072
- Ernst GGJ (1997) Dynamics of sediment-laden plumes. PhD Thesis, Department of Earth Sciences, University of Bristol, 223 pp
- Ernst GGJ, Davis JP, Sparks RSJ (1994) Bifurcation of volcanic plumes in a crosswind. *Bull Volcanol* 56:159–169
- Ernst GGJ, Sparks RSJ, Carey SN, Bursik MI (1996) Sedimentation from turbulent jets and plumes. *J Geophys Res* 101:5575–5589
- Giggenbach WF, Garcia PN, Londoño CA, Rodriguez VL, Rojas GN, Calvache VML (1990) The chemistry of fumarolic vapor and thermal spring discharges from the Nevado del Ruiz volcanic-magmatic-hydrothermal system. *J Volcanol Geotherm Res* 42:13–40
- Graedel TE, Crutzen PJ (1993) Atmospheric change: an earth system perspective. Freeman, New York, 446 pp
- Grindle TJ, Burcham FW (2002) Even minor volcanic ash encounters can cause major damage to aircraft. *ICAO J* 2:12–30
- Grönvold K, Larsen G, Einarsson P, Thórarinnsson S, Saemundsson K (1983) The Hekla eruption 1980–1981. *Bull Volcanol* 46:349–363
- Haraldsson KÖ (2001) Heklugosid 2000—Dreifing gjósku frá fyrsta gosdegi á landi (in Icelandic) (The Hekla 2000 eruption—distribution of ash from the first days of the eruption). BSc Thesis, University of Iceland, 34 pp
- Haraldsson KÖ, Árnason SG, Larsen G, Eiríksson J (2002) The Hekla eruption of 2000—tephra fall. In: Proc 25th Nordic Geological Winter Meeting, Reykjavík, Abstract
- Harris DM, Rose WI (1983) Estimating particles sizes, concentrations, and total mass of ash in volcanic clouds using weather radar. *J Geophys Res* 88:10969–10983
- Harris DM, Rose WI, Roe R, Thompson MR (1981) Radar observations of ash eruptions. In: Lipman PW, Mulineaux DR (eds) *The 1980 eruptions of Mount St. Helens*, Washington. US Geol Surv Prof Pap 1250:323–333
- Höskuldsson Á, Ólafsdóttir R (2002) Pyroclastic flows formed in the eruption of Hekla 2000. In: Proc 25th Nordic Geological Winter Meeting, Reykjavík, Abstract
- Houze RA (1993) Cloud dynamics. Academic Press, New York, 573 pp
- Karlsson KG (1997) An introduction to remote sensing in meteorology. Swedish Meteorological and Hydrological Institute, Norrköping, pp 95–129
- Krohn MD, Lemon LR, Perry J (1995) WSR-88D applications to volcanic ash detection. In: Proc 1st National NEXRAD Users Conf, Norman, Oklahoma, 11–15 Oct 1994
- Lacasse C (2001) Influence of climate variability on the atmospheric transport of Icelandic tephra in the subpolar North Atlantic. *Global Plan Change* 29:31–55
- Lacasse C, Thomas LE, Björnsson H, Gudmundsson MT, Gudmundsson H (2002) Potential hazards to Great Britain from major explosive eruptions: a cross-disciplinary study of the subglacial Katla volcano (S. Iceland). In: Proc Chapman Conf on Volcanism and the Earth's Atmosphere, Abstract, p 41
- Larsen G (2000) Holocene eruptions within the Katla volcanic system, south Iceland: characteristics and environmental impact. *Jökull* 49:1–28
- Larsen G, Vilmundardóttir EG, Thorkelsson B (1992) Heklugosid 1991: Gjóskufallid og gjósskulagid frá fyrsta degi gossins (in Icelandic) (The 1991 Hekla eruption: ash fall and ash layer from the first days of the eruption). *Náttúrufræðingurinn* 61(3–4):159–176
- McNutt SR (1994a) Volcanic tremor amplitude correlated with eruption explosivity and its potential use in determining ash hazards to aviation. In: Proc 1st Int Symp on Volcanic Ash and Aviation Safety. US Geol Surv Bull 2047:377–385

- McNutt SR (1994b) Volcanic tremor amplitude correlated with the Volcanic Explosivity Index and its potential use in determining ash hazards to aviation. *Acta Vulcanol* 5:193–196
- McNutt SR, Tytgat GC, Power JA (1995) Preliminary analyses of volcanic tremor associated with 1992 eruptions of Crater Peak, Mount Spurr, Alaska. *US Geol Surv* 2139:161–178
- Morton B, Taylor GI, Turner JS (1956) Turbulent gravitational convection from maintained and instantaneous source. *Proc R Soc Ser A* 234:1–23
- Ólafsdóttir R, Höskuldsson Á, Grönvold K (2002) The evolution of the lava flow from Hekla eruption 2000. In: *Proc 25th Nordic Geological Winter Meeting, Reykjavík*, Abstract
- Pieri D, Ma C, Simpson JJ, Hufford G, Grindle T, Grove C (2002) Analyses of in-situ airborne volcanic ash from the February 2000 eruption of Hekla volcano, Iceland. *Geophys Res Lett* 29(16)
- Probert-Jones JR (1962) The radar equation in meteorology. *Quat J R Met Soc* 88:485–495
- Rinehart R (1991) *Radar for meteorologists*, 2nd edn. Department of Atmospheric Sciences, University of North Dakota, Grand Forks, 334 pp
- Rose WI, Kostinski AB (1994) Radar remote sensing of volcanic clouds. In: *Proc 1st Int Symp on Volcanic Ash and Aviation Safety*. *US Geol Surv Bull* 2047:391–396
- Rose WI, Kostinski AB, Kelley L (1995a) Real-time C-band radar observations of 1992 eruption clouds from Crater Peak, Mount Spurr volcano, Alaska. *US Geol Surv Bull* 2139:19–26
- Rose WI, Delene DJ, Schneider DJ, Bluth GJS, Krueger AJ, Sprad I, McKee C, Davies HL, Ernst GGJ (1995b) Ice in the Rabaul eruption cloud: implications for volcano hazard and atmospheric effects. *Nature* 375:477–479
- Rose WI, Bluth GJ, Watson IM, Yu T, Gu Y (2001a) Hekla's February 26, 2000 eruption as seen and measured from space using MODIS, TOMS and AVHRR. In: *Proc AGU 2001 Fall Meeting*, Eos 82, F1355, Abstract
- Rose WI, Bluth GJ, Schneider DJ, Ernst GGJ, Riley CM, Henderson LJ, McGimsey RG (2001b) Observations of 1992 Crater Peak/Spurr volcanic clouds in their first few days of atmospheric residence. *J Geol* 109:677–694
- Rose WI, Gu Y, Watson IM, Yu T, Bluth GJS, Prata AJ, Krueger AJ, Krotkov N, Carn S, Fromm MD, Hundon DE, Viggiano AA, Miller TM, Ballentin JO, Ernst GGJ, Reeves JM, Wilson C, Anderson BE (2003) The February–March 2000 eruption of Hekla, Iceland, from a satellite perspective. In: Robock A, Oppenheimer C (eds) *Volcanism and the earth atmosphere*. AGU Geophys Monogr (in press)
- Soosalu H, Einarsson P (2002) Earthquake activity related to the 1991 eruption of the Hekla volcano, Iceland. *Bull Volcanol* 63:536–544
- Soosalu H, Einarsson P, Thorbjarnardóttir BS (2002) Volcanic tremor related to the 2000 Hekla eruption. In: *Proc Geol Soc Iceland, Spring Meeting*, Abstract
- Soosalu H, Einarsson P, Jakobsdóttir S (2003) Volcanic tremor related to the 1991 eruption of the Hekla volcano, Iceland. *Bull Volcanol* 65:562–577
- Sparks RSJ, Bursik, MI, Carey SN, Gilbert JS, Glaze LS, Sigurdsson H, Woods AW (1997) *Volcanic plumes*. Wiley, Chichester, 574 pp
- Stefánsson R, Bödvarsson R, Slunga R, Einarsson P, Jakobsdóttir S, Bungum H, Gregersen S, Havskov J, Hjelme J, Korhonen H (1993) Earthquake prediction research in the South Iceland Seismic Zone and the SIL project. *Bull Seismol Soc Am* 83:696–716
- Sveinbjörnsson M (2001) Volcanic eruptions in Iceland: potential hazards and aviation safety. MSc Thesis, University of Iceland, 71 pp
- Textor C, Graf H-F, Herzog M, Oberhuber JM, Rose WI, Ernst GGJ (2003a) Volcanic particles in explosive eruption columns. Part I: parameterisation of ash aggregation. *J Volcanol Geotherm Res* (in press)
- Textor C, Graf H-F, Herzog M, Oberhuber JM, Rose WI, Ernst GGJ (2003b) Hydrometeor-ash particle growth in volcanic eruption column. Part II: numerical experiments. *J Volcanol Geotherm Res* (in press)
- Thórarinnsson S (1954) The tephra fall from Hekla on March 29th 1947. The eruption of Hekla 1947–1948. *Soc Sci Islandica* 2(3):68
- Thórdarson Th, Self S (2003) Atmospheric and environmental effects of the 1783–1784 Laki eruption: a review and reassessment. *J Geophys Res* 108(D1)
- Wilson L (1972) Explosive volcanic eruptions—II: the atmospheric trajectories of pyroclasts. *Geophys J R Astron Soc* 30:381–392